
Coherent Control of Stimulated Emission Inside one Dimensional Photonic Crystals – Strong Coupling Regime

Alessandro Settimi

Additional information is available at the end of the chapter

<http://dx.doi.org/10.5772/59900>

1. Introduction

It is well known that emission processes reflect certain inherent properties of atoms, but it has also been demonstrated, in both theory [1,2] and experimentation [3-8], that these same processes are also sensitive to incidental boundary conditions. One example is how they can be modified if contained inside a cavity of dimensions comparable to the emitted light wavelength. The modification can involve emission enhancement or inhibition and is a result of an alteration of field mode structure inside the cavity compared to free space, which can be explained in terms of an interaction between atom and cavity modes [9,10].

The density of states (DOS) can be interpreted as a probability density of exciting a single eigenstate of the electromagnetic (e.m.) field. When the plot of DOS vs. frequency over atomic transition spectral range is found to be smooth, then the rate of emission can be defined by Fermi's golden rule. However, emission dynamics can be drastically modified by photon localization effects [11] and sudden changes in DOS. Such modifications can be interpreted as long-term memory effects and examples of non-Markovian atom-reservoir interactions.

Marked transformations can be induced in the DOS using photonic crystals. These dielectric materials exhibit very noticeable periodic modulations in their refractive indices which result in the formation of inhibited [12,13] frequency bands or photonic band gaps. The DOS inside a photonic band gap (PBG) is automatically zero. It is proposed in literature [14-17] that these conditions might result in classical light localization, inhibition of single-photon emissions, fractionalized single-atom inversions, photon-atom bound states, and anomalously strong vacuum Rabi splitting.

There have been rigorous investigations of spontaneous decay of two-level atoms coupled with narrow cavity resonance according to Hermitian "universal" modes as against the dissipative quasi-modes of the cavity by reference [18]. These have concentrated in particular on cases in which the atomic line-width is nearly equal to the cavity resonance width γ , the so-called strong-coupling regime, when significant corrections are found into the golden rule. When the quality factor Q of cavity resonance falls within intermediate values, then spontaneous emission is seen to decay rapidly.

The emission processes investigated in this chapter regard a 1D unenclosed cavity, analysed according to the theory of reference [18]. There is specific discussion of the stimulated release of an atom under strong coupling regime inside a 1D-PBG cavity generated by two colliding laser beams. Atom-e.m. field coupling is modelled by quantum electro-dynamics, as per reference [18], with the atom considered as a two tier system, and the e.m. field as a superposition of normal modes. The coupling is in dipole approximation, Wigner-Weisskopf and rotating wave approximations are applied for the motion equations. An unenclosed cavity is conceived in the Quasi-Normal Mode (QNM), as in reference [18], and so the local density of states (LDOS) is defined as the local probability density of exciting a single cavity QNM. As a result the local DOS is effectively dependent on the phase difference between the two laser beams.

1.1. Quasi-Normal Modes (QNMs)

Describing a field inside an unenclosed cavity presents a problem that various authors have confronted, with references [19-22] proposing a QNM-based description of an electromagnetic field inside an open, one-sided homogeneous cavity. Because of the leakage, the QNMs exhibit complex eigen-frequencies as a consequence of leakage from the unenclosed cavity, with an orthogonal basis being assumed only inside the cavity and following a non-canonical metric.

The QNM approach was extended to open double-sided, non-homogeneous cavities and specifically to 1D-PBG cavities in references [23,24].

It is only possible to quantize a leaky cavity [25], considered a dissipative system, if the container is viewed as part of the total universe, within which energy is conserved [26]. A fundamental step towards the application of QNMs to the study of quantum electro-dynamics phenomena in cavities was already achieved in reference [27].

The second QNM-theory-based quantization scheme was extended to 1D-PBGs in reference [28]. References [29,30] applied the second QNM quantization to 1D-PBGs, excited by two pumps acting in opposite directions. The commutation relations observed for QNMs are not canonical, while also depending on the phase-difference between the two pumps and the unenclosed cavity geometry. Reference [31] applies QNM theory in an investigation of stimulated emission from an atom embedded inside a 1D-PBG under weak coupling regime, with two counter-propagating laser beams used to pump the system. The most significant result in reference [31] is the observation that the position of the dipole inside the cavity controls decay-time. This means that the phase-difference of the two laser beams can be used to control decay-time, which could be applicable on an atomic scale for a phase-sensitive, single-atom optical memory device.

The present chapter discusses stimulated emission of an atom enclosed inside a 1D-PBG cavity under strong coupling regime, generated by two counter-propagating laser beams [32,33]. The principal observation is a demonstration that high LDOS values can be used as a definition for a strong coupling regime. Further observations agree with literature in stating that the atomic emission probability decays with an oscillating pattern, and the atomic emission spectrum split into two peaks, known as Rabi splitting. What makes the observations of this chapter unique compared to literature is that by varying the laser beam phase difference it is possible to effectively control both the atomic emission probability oscillations, and the characteristic Rabi splitting of the emission spectrum. Some criteria are proposed for the design of active cavities, comprising a 1D-PBG together with atom, as active delay line, when it is possible to achieve high transmission in a narrow pass band for a delayed pulse by applying suitably differing laser beams phases.

In section 2, quantum electro-dynamic equations are used to model the coupling of an atom to an e.m. field, as an analogy of the theory of an atom in free space. In section 3, the atom is also contained within an unenclosed cavity, and the local probability density of a single QNM being excited is considered a definition of LDOS probability density. The atomic emission processes are modelled in section 4 with the LDOS of the stimulated emission depending on the phase difference of two counter-propagating laser beams. Section 5 discusses the probability of atomic emission under strong coupling regime. In section 6, the atomic emission spectrum is defined on the basis of its poles. Some criteria for the design of an active delay line are proposed in section 7, while section 8 is dedicated to a final discussion and concluding remarks.

2. Coupling of an atom to an electromagnetic (e.m.) field

The present case study examines an atom coupled to an e.m. field at a point $x_0 \in U$ inside a one-dimensional (1D) universe $U = \{x \mid x \in [-L/2, L/2], L \rightarrow \infty\}$ with refractive index n_0 , and an unenclosed cavity $C = \{x \mid x \in (0, d), d < L\}$ with an inhomogeneous refractive index $n(x)$.

The atom is quantized into two levels, with an oscillating resonance of Ω [25]. The 1D universe modes are applied to quantize the e.m. field

$$\begin{cases} g_\lambda(x) = \frac{1}{\sqrt{L}} \exp(i\omega_\lambda \sqrt{\rho_0} x) \\ \omega_\lambda = \lambda \frac{\pi}{(L/2)\sqrt{\rho_0}}, \quad \lambda \in \mathbb{Z} \end{cases} \quad (1)$$

when $\rho_0 = (n_0/c)^2$, and c is the speed of light in a vacuum. The dipole operator μ [25] is used to model the atom along the direction of polarization of the e.m. field, and the coupling of the atom to the e.m. field is described using the electric dipole approximation [26].

At start time ($t=0$) the atom is in an excited state $|+\rangle$ and the e.m. field is in a vacuum state $| \{0\} \rangle = \prod_{\lambda=-\infty}^{\infty} |0_{\lambda}\rangle$. The system dynamics under these initial conditions can be described with basis states and corresponding eigen-values [18] as follows:

$$\begin{aligned} |+\{0\}\rangle &= |+\rangle | \{0\} \rangle, \quad \varepsilon_+ \\ |-\{1_{\lambda}\}\rangle &= |-\rangle |1_{\lambda}\rangle, \quad \varepsilon_- + \hbar\omega_{\lambda}, \quad \lambda \in \mathbb{Z}. \end{aligned} \tag{2}$$

when $|+\{0\}\rangle$ denotes the upper state of the atom, without any photons in all the e.m. modes; and $|-\{1_{\lambda}\}\rangle$ denotes the lower state of the atom, with one photon in the λ^{th} e.m. mode but any photons in the other e.m. modes.

2.1. Quantum electro-dynamic equations

If an initial condition $|+\{0\}\rangle$ is assumed, then the atom-field system state at time instant $t>0$ can be defined as

$$|\psi(t)\rangle = c_+(t)|+\{0\}\rangle + \sum_{\lambda=-\infty}^{\infty} c_{-\lambda}(t)|-\{1_{\lambda}\}\rangle, \tag{3}$$

introducing the probability amplitudes $c_+(t)$ and $c_{-\lambda}(t)$ with $c_+(0)=1$ and $c_{-\lambda}(0)=0$, and assuming the rotating wave approximation [26]. The time evolution equations for the probability amplitudes $c_+(t)$ and $c_{-\lambda}(t)$ [18] are used as a starting point, thus

$$\begin{aligned} \frac{dc_+}{dt} &= \frac{\langle +|\mu|-\rangle}{\hbar} \sum_{\lambda=1}^{\infty} \sqrt{\frac{\hbar\omega_{\lambda}}{2\varepsilon_0 n_0^2}} g_{\lambda}(x_0) c_{-\lambda}(t) \exp[-i(\omega_{\lambda} - \Omega)t] \\ \frac{dc_{-\lambda}}{dt} &= -\frac{\langle -|\mu|+\rangle}{\hbar} \sqrt{\frac{\hbar\omega_{\lambda}}{2\varepsilon_0 n_0^2}} g_{\lambda}^*(x_0) c_+(t) \exp[i(\omega_{\lambda} - \Omega)t], \end{aligned} \tag{4}$$

the second of these can be formally integrated producing a time evolution equation for the probability amplitude $c_+(t)$ as follows:

$$\frac{dc_+}{dt} = -\frac{M}{2\varepsilon_0 n_0^2 \hbar^2 L} \sum_{\lambda=1}^{\infty} \hbar\omega_{\lambda} \int_0^t c_+(\tau) \exp[i(\omega_{\lambda} - \Omega)(\tau - t)] d\tau. \tag{5}$$

when ε_0 is the dielectric constant in vacuum and $M = |\langle +|\mu|-\rangle|^2$.

It is possible to establish a correspondence between the discrete modes and continuous modes of, respectively, a 1D cavity of length L , and an infinite universe of length $L \rightarrow \infty$. As $L \rightarrow \infty$,

the mode spectrum approaches continuity, since $\Delta\omega_\lambda = \pi / (L/2)\sqrt{\rho_0} \approx d\omega \rightarrow 0$. When this limit is reached, sums over discrete indices can be transformed into integrals over a continuous variable of frequency,

$$\frac{1}{L} \sum_{\lambda=1}^{\infty} \Rightarrow \int_0^{\infty} d\omega \sigma^{(\text{loc})}(x_0, \omega), \quad (6)$$

when $\sigma^{(\text{loc})}(x, \omega)$ is the local density of states (LDOS), which can be interpreted as the density of probability for an excited level of the e.m. field, at a point x , collapsed into a single eigen-state, oscillating around the frequency ω [34,35]. Strictly speaking, in Equation (6), the range of integration over ω only extends from 0 to ∞ , given that the physical frequencies are defined as positive. Nevertheless, it is possible to extend the range from $-\infty$ to ∞ without significant errors, due to the fact that most optical experiments utilize a narrow band source B [36], such that $B \ll \omega_c$ with ω_c the bandwidth B as the central frequency. The time evolution Equation (5) therefore becomes

$$\frac{dc_{\pm}}{dt} = \int_0^t d\tau \cdot K(x_0, t - \tau) c_{\pm}(\tau), \quad (7)$$

the kernel function $K(x, t)$ being defined as:

$$K(x, t) = -\frac{M}{2\epsilon_0 n_0^2 \hbar^2} \int_{-\infty}^{\infty} d\omega \hbar \omega \sigma^{(\text{loc})}(x, \omega) \exp[-i(\omega - \Omega)t]. \quad (8)$$

As emerges from Equation (8), there is a marked dependence of the kernel function on the LDOS through $\sigma^{(\text{loc})}(x, \omega)$. It is possible to reinterpret the latter as the density of photon states in the reservoir. Essentially, the kernel function (8) is a gauge of the memory of previous state of the photon reservoir, within the evolutionary time scale of the atomic system, thus $K(x, t)$ could be considered the photon reservoir's memory kernel.

2.2. Atom in free space

If an atom is located at a given point x_0 outside the unenclosed cavity, so that $x_0 < 0$ or $x_0 > d$, then the local DOS $\sigma^{(\text{loc})}(x, \omega)$ refers to free space (see references [26,31]):

$$\sigma^{(\text{loc})}(x, \omega) = \sigma_{\text{free-space}}(\omega) = \sigma_{\text{ref}} = \frac{\sqrt{\rho_0}}{2\pi}. \quad (9)$$

The probability of atomic emission decays exponentially in free space,

$$|c_+(t)|^2 = \exp(-\Gamma_0 t) \quad , \quad t \geq 0, \quad (10)$$

being Γ_0 the atomic decay rate:

$$\Gamma_0 = \frac{M \sqrt{\rho_0}}{\hbar \varepsilon_0 n_0^2} \Omega \left/ \left[1 + \frac{1}{4} \left(\frac{M \sqrt{\rho_0}}{\hbar \varepsilon_0 n_0^2} \right)^2 \right] \right. \quad (11)$$

Free space is an infinitely large photon reservoir (a flat spectrum), and so it should respond instantaneous, with any memory effects associated to emission dynamics being infinitesimally short relative to any time intervals of interest. According to the so-called Markovian [26] interactions, an excited state population gradually decays to ground level in free space, regardless of any driving field strength. This result is generally valid for almost any smoothly varying broadband DOS.

The following parameter is now introduced as a step for the analysis of the next section,

$$R = \frac{\Gamma_0}{\Omega} \cong \frac{M \sqrt{\rho_0}}{\hbar \varepsilon_0 n_0^2}, \quad (12)$$

interpretable as the degree of atom-field coupling, and with the possibility of expressing Equation (8) as:

$$K(x, t) = -\frac{R}{2\sqrt{\rho_0}} \int_{-\infty}^{\infty} d\omega \cdot \omega \sigma^{(\text{loc})}(x, \omega) \exp[-i(\omega - \Omega)t]. \quad (13)$$

3. Atom inside an unenclosed cavity

Assuming $0 < x_0 < d$, which represents an atom embedded at a point x_0 inside an open, inhomogeneous cavity with refractive index $n(x)$, if the resonance frequency Ω of the atom is coupled with the n^{th} QNM oscillating at frequency $\text{Re}\omega_n$, then the coupling will exhibit frequency detuning:

$$\Delta_n = \frac{\text{Re}\omega_n - \Omega}{R}. \quad (14)$$

3.1. Density Of States (DOS) as the probability density to excite a single QNM

By filtering two counter-propagating pumps at an atomic resonance $\Omega \approx \text{Re}\omega_n$, it emerges that only the n^{th} QNM, and no other QNMs, can be excited, because the n^{th} QNM is the only one

oscillating at the frequency $\text{Re}\omega_n$ and within the narrow range $2|\text{Im}\omega_n| \ll |\text{Re}\omega_n|$, which is sufficiently remote to exclude the other QNMs [23,24]. Around point x , the local probability density that the e.m. field is in fact excited on the n^{th} QNM is [31]

$$\sigma_n^{(\text{loc})}(x, \omega) = \frac{1}{I_n} \sigma_n(\omega) \rho(x) |f_n^N(x)|^2, \quad \forall x | 0 < x < d, \quad (15)$$

which is related directly to the (integral) probability density $\sigma_n(\omega)$ for the n^{th} QNM. In Equation (15), $\rho(x) = [n(x)/c]^2$, I_n denotes an appropriate overlapping integral [28], while $f_n^N(x) = f_n(x) \sqrt{2\omega_n} / \langle f_n | f_n \rangle$ is the normalized QNM function, with $\langle f_n | f_n \rangle$ representing the QNM norm.

For the investigation of spontaneous emissions, the two pumps are modelled as fluctuations of vacuum, based on the e.m. field ground state (for examples, see references [26,28-30]). The (integral) probability density that the n^{th} QNM is excited within the unenclosed cavity can be expressed as [31]:

$$\sigma_n^{(1)}(\omega) = \frac{1}{d} \int_0^d \sigma_n^{(1)}(x, \omega) dx = \alpha_n \frac{d}{2\pi} \frac{I_n^2 |\text{Im}\omega_n|}{(\omega - \text{Re}\omega_n)^2 + \text{Im}^2 \omega_n}. \quad (16)$$

It is possible to deduce a normalization constant α_n from the condition:

$$\int_{\text{Re}\omega_n - |\text{Im}\omega_n|}^{\text{Re}\omega_n + |\text{Im}\omega_n|} \sigma_n^{(1)}(\omega) d\omega + \int_{-\text{Re}\omega_n - |\text{Im}\omega_n|}^{-\text{Re}\omega_n + |\text{Im}\omega_n|} \sigma_n^{(1)}(\omega) d\omega = \frac{1}{d}. \quad (17)$$

From Equation (16) it was deduced that the probability density due to fluctuations in vacuum for the n^{th} QNM is a Lorentzian function, with parameters including real and imaginary parts of the n^{th} QNM frequency. There is a relation between the overlapping integral I_n and the statistical weight of the n^{th} QNM in the DOS. Equation (17) also integrates the probability density $\sigma_n^{(1)}(\omega)$ into the range of negative frequencies $\omega \in [-\text{Re}\omega_n - |\text{Im}\omega_n|, -\text{Re}\omega_n + |\text{Im}\omega_n|]$, since with $\text{Re}\omega_n > 0$ the QNM frequency ω_n is also represented by frequency $\omega_{-n} = -\omega_n^*$ with $\text{Re}\omega_{-n} < 0$ [23,24].

Stimulated emissions are considered by modelling the two pumps as a pair of laser beams in a coherent state (see references [26,28-30] for examples). When the symmetry property is achieved by the refractive index $n(x)$, so that $n(d/2-x) = n(d/2+x)$, then the probability density that the e.m. field is excited to the n^{th} QNM inside the cavity can be written as [31]:

$$\sigma_n^{(\text{II})}(\omega) = \sigma_n^{(1)}(\omega) \left[\Delta + (-1)^n \cos \varphi \right] \quad (18)$$

Equation (18) shows that the phase-difference $\Delta\varphi$ of the pair of counter-propagating laser beams can be used to control the probability density for the n^{th} QNM.

4. Atomic emission processes

With an atom at point x_0 of an unenclosed inhomogeneous cavity, so that $0 < x_0 < d$, and electromagnetic field coupling limited to the n^{th} QNM $[\omega_n, f_n^{\text{N}}(x)]$ of the unenclosed cavity, then the local probability density $\sigma_n^{(\text{loc})}(x, \omega)$ is related to the integral probability density $\sigma_n(\omega)$ as in Equation (15) and the atomic emission processes exhibit a characteristic kernel function $K(x, t)$, which can be expanded as [see Equation (13)]:

$$K_n(x, t) = -\frac{R}{2\sqrt{\rho_0}} \frac{1}{I_n} \rho(x) |f_n^{\text{N}}(x)|^2 \int_{-\infty}^{\infty} d\omega \cdot \omega \sigma_n(\omega) \exp[-i(\omega - \Omega)t], \quad \forall x | 0 < x < d. \quad (19)$$

4.1. Spontaneous emission: DOS due to vacuum fluctuations

If the unenclosed cavity is only affected by fluctuations of vacuum filtered at the atomic resonance Ω and close to the cavity's n^{th} QNM frequency ($\Omega \approx \text{Re}\omega_n$), then Equations (16) and (17) can be used to express the integral probability density $\sigma_n^{(1)}(\omega)$ for the n^{th} QNM, and atomic spontaneous emission exhibits a characteristic time evolution [see Equation (7)] in which the kernel function $K_n(x, t)$ can be expressed as [see Equation (19)]:

$$K_n^{(1)}(x, t) = -\frac{R}{2\sqrt{\rho_0}} \frac{1}{I_n} \rho(x) |f_n^{\text{N}}(x)|^2 \alpha_n \frac{d}{2\pi} I_n^2 \exp(i\Omega t) \cdot \cdot i\sqrt{2\pi} \left[\frac{1}{\sqrt{2\pi}} \int_{-\infty}^{\infty} (-i\omega) \frac{|\text{Im}\omega_n|}{(\omega - \text{Re}\omega_n)^2 + \text{Im}^2\omega_n} \exp(-i\omega t) d\omega \right]. \quad (20)$$

The resulting signal $x(t)$ can easily be transformed into the Fourier domain [37]:

$$x(t) = \frac{1}{2} \frac{d}{dt} \left[e^{-(|\text{Im}\omega_n| + i\text{Re}\omega_n)|t|} \right] \\ \Rightarrow X(\omega) = \frac{1}{\sqrt{2\pi}} \int_{-\infty}^{\infty} x(t) \exp(i\omega t) dt = -\frac{i\omega}{\sqrt{2\pi}} \frac{|\text{Im}\omega_n|}{\text{Im}^2\omega_n + (\omega - \text{Re}\omega_n)^2}. \quad (21)$$

Applying Equations (20) and (21) for the kernel function of the spontaneous emission process gives:

$$K_n^{(1)}(x, t) = -\frac{1}{4} \frac{R}{\sqrt{\rho_0}} \alpha_n (d \cdot I_n) \omega_n \rho(x) |f_n^{\text{N}}(x)|^2 \exp[-i(\omega_n - \Omega)t], \quad \forall t \geq 0. \quad (22)$$

Now, in Equation (7), deriving under the integral sign [37] gives

$$\frac{d^2 c_+}{dt^2} = K_n^{(1)}(x_0, t=0)c_+(t) + \int_0^t d\tau \frac{\partial K_n^{(1)}}{\partial t} c_+(\tau), \quad (23)$$

and deriving Equation (22) again, sampled at point x_0 , relative to time,

$$\frac{\partial K_n^{(1)}}{\partial t} = -i(\omega_n - \Omega)K_n^{(1)}(x_0, t) \quad , \quad t \geq 0, \quad (24)$$

which after some algebraic transformations produces a second order differential equation in time for spontaneous emission probability:

$$\begin{aligned} \frac{d^2 c_+}{dt^2} + i(\omega_n - \Omega) \frac{dc_+}{dt} - K_n^{(1)}(x_0, t=0)c_+(t) &= 0 \\ c_+(0) = 1 \quad , \quad \left. \frac{dc_+}{dt} \right|_{t=0} &\propto c_{-,n}(0) = 0. \end{aligned} \quad (25)$$

4.2. Stimulated emission: DOS dependant on the phase difference of a pair of counter-propagating laser-beams

If the unenclosed cavity is pumped coherently by two counter-propagating laser beams with a phase difference $\Delta\varphi$, tuned to the atomic resonance Ω and closed to the n^{th} QNM frequency ($\Omega \approx \text{Re}\omega_n$), then the probability density $\sigma_n^{(\text{II})}(\omega)$ for the n^{th} QNM, for the state of the two laser beams, is related to $\sigma_n^{(\text{I})}(\omega)$, which is calculated using Equation (18) when vacuum fluctuations are present. The atomic stimulated emission exhibits a characteristic kernel function $K_n(x, \omega)$, which can be expressed as follows [see Equation (20)]:

$$K_n^{(\text{II})}(x, t) = K_n^{(\text{I})}(x, t) \left[1 + (-1)^n \cos \Delta\varphi \right]. \quad (26)$$

The quantity $(\omega_n - \Omega)$ can be re-expressed in terms of frequency detuning (14), as $(\omega_n - \Omega) = (\text{Re}\omega_n - \Omega) + i\text{Im}\omega_n = R\Delta_n + i\text{Im}\omega_n$ so that the second order differential equation for emission probability becomes:

$$\frac{d^2 c_+}{dt^2} + i(R\Delta_n + i\text{Im}\omega_n) \frac{dc_+}{dt} - K_n(x_0, t=0)c_+(t) = 0 \quad (27)$$

5. Atomic emission probability

The initial conditions being the same as Equation (25), the algebraic equation associated with the Cauchy problem (27) can be recast as:

$$p^2 + (R\Delta_n + i \operatorname{Im} \omega_n) p + K_n(x_0, t = 0) = 0. \quad (28)$$

This is solved with two roots,

$$p_{1,2} = \frac{(R\Delta_n + i \operatorname{Im} \omega_n)}{2} \left[-1 \pm \sqrt{1 - \frac{4K_n(x_0, t = 0)}{(R\Delta_n + i \operatorname{Im} \omega_n)^2}} \right], \quad (29)$$

which permit expression of the particular integral of the differential Equation (27) as:

$$c_+(t) = \frac{p_2}{p_2 - p_1} \exp(ip_1 t) - \frac{p_1}{p_2 - p_1} \exp(ip_2 t). \quad (30)$$

The atom and the n^{th} QNM are coupled under a strong regime when the behaviour of the particular integral (30) is oscillatory, and when the two roots (29) of the relative algebraic Equation (28), are complex conjugates [18].

5.1. Strong coupling regime

Spontaneous emission is examined in order to assess the atom - n^{th} QNM coupling under strong regime. Given that,

$$4 \left| \frac{K_n^{(1)}(x_0, t = 0)}{(R\Delta_n + i \operatorname{Im} \omega_n)^2} \right| < \frac{R}{d \cdot I_n} \frac{\sigma_n^{(1)}(x_0, \Omega)}{\sigma_{\text{free-space}}} \cong R \frac{\sigma_n^{(1)}(x_0, \Omega)}{\sigma_{\text{free-space}}}, \quad (31)$$

there is a strong coupling regime if [18]:

$$4 \left| \frac{K_n(x_0, t = 0)}{(R\Delta_n + i \operatorname{Im} \omega_n)^2} \right| > 1 \Rightarrow \frac{\sigma_n^{(1)}(x_0, \Omega)}{\sigma_{\text{free-space}}} > \frac{1}{R}. \quad (32)$$

Equation (32) shows that a strong coupling regime is present when the probability density (16) inside the unenclosed cavity, sampled at atomic resonance in units of DOS (9) with reference to free space, is in excess of the inverse of the atomic parameter R [see Equation (12)]. An interpretation of parameter R as a level of atom field coupling is thus legitimated: the greater R becomes, the better Equation (32) is satisfied. The two roots (29) become complex conjugates in the hypothesis of a strong coupling regime (32),

$$p_{1,2} \cong -\frac{R\Delta_n + i \operatorname{Im} \omega_n}{2} \pm i \sqrt{K_n^{(1)}(x_0, t = 0)}, \quad (33)$$

and the behaviour of the particular integral (30) is oscillatory:

$$c_+(t) \cong \exp\left(-i\frac{R\Delta_n + i\text{Im}\omega_n}{2}t\right) \cdot \left\{ \cosh\left[\sqrt{K_n^{(I)}}(x_0, t=0)t\right] + i\frac{R\Delta_n + i\text{Im}\omega_n}{2\sqrt{K_n^{(I)}}(x_0, t=0)} \sinh\left[\sqrt{K_n^{(I)}}(x_0, t=0)t\right] \right\} \quad (34)$$

In reality [see Equation (22)] $K_n^{(I)}(x_0, t=0) = -K_n^{(II)}(x_0, t=0)$. It is possible to interpret the oscillatory behaviour as emission re-absorption of a single photon and so the net decay rate can thus be determined from the rate of photon leakage, which is $|\text{Im}\omega_n|/2$.

In the case of stimulated emissions, the coupling between atom and the n^{th} QNM can again be considered under strong regime. Given a phase difference of $\Delta\varphi$ for the pair of counter-propagating laser beams, then the atom - n^{th} QNM coupling exhibits the kernel function (26). Assuming hypothetical strong coupling as expressed by a similar condition to Equation (32), the behaviour of the particular integral (30) is oscillatory,

$$c_+(t) \cong \exp\left(-i\frac{R\Delta_n + i\text{Im}\omega_n}{2}t\right) \cdot \left\{ \cosh\left[\sqrt{K_n^{(II)}}(x_0, t=0)t\right] + i\frac{R\Delta_n + i\text{Im}\omega_n}{2\sqrt{K_n^{(II)}}(x_0, t=0)} \sinh\left[\sqrt{K_n^{(II)}}(x_0, t=0)t\right] \right\}, \quad (35)$$

when $K_n^{(II)}(x_0, t=0)$ is linked to the phase difference $\Delta\varphi$ through Equation (26). The quantity of atomic emission probability oscillations is dependent on the position of the atom inside the cavity and so the phase-difference of the paired laser-beams can be used to control it. The condition,

$$1 + (-1)^n \cos\Delta\varphi = 0, \quad (36)$$

is satisfied if the atom is coupled to an odd QNM, i.e. $n=1,3,\dots$ and the paired laser beams are in phase, i.e. $\Delta\varphi=0$; or if the atom is coupled to an even QNM, i.e. $n=0,2,\dots$ and the paired laser beams are out of phase, i.e. $\Delta\varphi=\pi$. When Equation (36) is satisfied, the probability of emission is over-damped within the entire cavity. Even under strong coupling, no oscillation occurs [see Equation (35)]:

$$K_n^{(II)}(x_0, t=0) = 0 \Rightarrow |b_+(t)|^2 = \exp\left(\frac{|\text{Im}\omega_n|^2}{4}t\right) \left[\left(1 + \frac{|\text{Im}\omega_n|}{2}t\right)^2 + \left(\frac{R\Delta_n}{2}t\right)^2 \right]. \quad (37)$$

6. Atomic emission spectrum

An atom located at point x_0 is in its upper state at initial time ($t=0$) and there are no photons present in any normal mode, i.e. $c_+(x_0, t=0)=1$. Following atomic decay ($t=\infty$), Equation (4) can be used to derive the coefficient of probability $c_{-, \lambda}(x_0, t)$ of finding the atom in its lower state with one photon in the λ^{th} e.m. mode and no photons in all the other modes:

$$c_{-, \lambda}(x_0, t = \infty) = -\frac{\langle -|\mu|+ \rangle}{\hbar} \sqrt{\frac{\hbar \omega_\lambda}{2 \varepsilon_0 n_0^2}} g_\lambda^*(x_0) \int_0^\infty c_+(x_0, t) \exp[i(\omega_\lambda - \Omega)t] dt. \quad (38)$$

Applying the Laplace transform for probability coefficient $c_+(x_0, t)$,

$$C_+(x_0, s) = \frac{1}{\sqrt{2\pi}} \int_0^\infty c_+(x_0, t) \exp(-st) dt, \quad (39)$$

Equation (38) can thus be re-formulated as:

$$c_{-, \lambda}(x_0, t = \infty) = -\frac{\langle -|\mu|+ \rangle}{\hbar} \sqrt{\frac{\hbar \omega_\lambda}{2 \varepsilon_0 n_0^2}} g_\lambda^*(x_0) \sqrt{2\pi} C_+[x_0, s = i(\omega_\lambda - \Omega)]. \quad (40)$$

If decay has occurred ($t=\infty$), it is possible to define the atomic emission spectrum as the probability density that the atom at point x_0 emitted at frequency ω [18], i.e.

$$W(x_0, \omega) = \sum_{\lambda=1}^\infty |c_{-, \lambda}(x_0, t = \infty)|^2 \delta(\omega - \omega_\lambda), \quad (41)$$

when $\delta(t)$ is the Dirac delta distribution. Integrating Equation (40) into Equation (41), gives:

$$W(x_0, \omega) = \frac{M}{2 \varepsilon_0 n_0^2 \hbar^2} \frac{1}{L} \sum_{\lambda=1}^\infty \hbar \omega_\lambda 2\pi |C_+[x_0, i(\omega_\lambda - \Omega)]|^2 \delta(\omega - \omega_\lambda). \quad (42)$$

If sums over discrete quantities are converted to integrals over continuous frequencies, using Equation (6), then the Dirac delta properties can be used to reduce the emission spectrum (42) to:

$$W(x_0, \omega) = \alpha' \cdot \frac{R}{2\sqrt{\rho_0}} \omega \sigma^{(\text{loc})}(x_0, \omega) 2\pi |C_+[x_0, i(\omega - \Omega)]|^2, \quad (43)$$

when α' is a suitable normalization constant and $\sigma^{(\text{loc})}(x, \omega)$ is the local density of states (DOS). Equation (12) is used to define the atomic parameter R .

Given that most optical experiments apply a narrow band source [36], it is possible to extend the frequency range from $-\infty$ to ∞ without significant errors, and the closure relation can be applied to establish the normalization constant α'

$$\int_{-\infty}^{\infty} W(x_0, \omega) d\omega = 1, \tag{44}$$

which derives directly from the interpretation of emission spectrum probability (43). Assuming $0 < x_0 < d$ and $n(x_0) > n_0$, the atom is embedded inside an unenclosed cavity with inhomogeneous refractive index $\rho(x) = [n(x)/c]^2$. The atom with resonance frequency Ω can be assumed coupled to the n^{th} QNM and oscillating at the frequency $\text{Re}\omega_n$. This atom to n^{th} QNM coupling is characterized by frequency detuning Δ_n (14). The normalization condition (44) can be reduced to:

$$2 \int_{\Omega - |\text{Im}\omega_n|}^{\Omega + |\text{Im}\omega_n|} W_n(x_0, \omega) d\omega = 1. \tag{45}$$

Integrals over positive frequencies are multiplied by a factor of 2 in Equation (45) in order to include the contribution of negative frequencies [see comments following Equation (17)].

Equation (15) showed that the local probability density $\sigma_n^{(\text{loc})}(x, \omega)$ for the n^{th} QNM was proportional to $\sigma_n(\omega)$. Now if Equation (15) is included into Equation (43), the atomic emission spectrum is expressed as

$$W_n(x_0, \omega) = \alpha'_n \cdot \frac{R}{2\sqrt{\rho_0}} \frac{1}{I_n} \rho(x_0) |f_n^{(N)}(x_0)|^2 \omega \sigma_n(\omega) 2\pi |C_+^{(n)}[x_0, i(\omega - \Omega)]|^2, \tag{46}$$

when α'_n is the normalization constant that satisfies Equation (45).

The atomic emission processes exhibit a characteristic kernel function $K_n(x, t)$, here expressible as in Equation (22), while for stimulated emission as in Equation (26). By including Equation (22) into Equation (46), the emission spectrum (46) assumes the form:

$$\frac{W_n(x_0, \omega)}{\alpha'_n} = - \frac{2}{d \cdot I_n^2} \frac{K_n^{(1)}(x_0, t=0)}{\omega_n} \omega \frac{\sigma_n(\omega)}{K_n} 2\pi |C_+^{(n)}[x_0, i(\omega - \Omega)]|^2. \tag{47}$$

The emission spectrum $W_n(x_0, \omega)$ emerging from Equation (47) depends on both the probability density $\sigma_n(\omega)$, and the initial kernel function value $K_n^{(1)}(x_0, t=0)$.

Now, by applying the Laplace transformation of the Cauchy problem (27), and the initial conditions derived from Equation (25), gives finally [37]

$$C_+^{(n)}(x_0, i\xi) = -\frac{i}{\sqrt{2\pi}} \frac{\xi + R\Delta_n + i \operatorname{Im} \omega_n}{\xi^2 + (R\Delta_n + i \operatorname{Im} \omega_n)\xi + K_n(x_0, t=0)}, \quad (48)$$

when ξ is the shifted frequency $(\omega - \Omega)$, with Ω denoting atomic resonance.

6.1. Poles of the emission spectrum

The two poles that solve Equation (28), p_1 and p_2 , can be used to describe the atomic emission spectrum, as expressed in Equation (29). Hypothesizing a strong coupling regime [see Equation (32)], the atomic emission spectrum $W_n(x_0, \xi)$ as a function of the shifted frequency $\xi = (\omega - \Omega)$, exhibits two characteristic peaks, centred approximately in the $\operatorname{Re} p_1$ and $\operatorname{Re} p_2$ resonances with bandwidths linked to $2 | \operatorname{Im} p_1 |$ and $2 | \operatorname{Im} p_2 |$. There is thus a Rabi splitting with the two peaks separated by:

$$\Delta\xi = \operatorname{Re} p_1 - \operatorname{Re} p_2. \quad (49)$$

Considering stimulated emission processes, the paired counter-propagating laser beams are set to a phase difference $\Delta\varphi$, and so the emission spectrum $W_n(x_0, \xi)$ can be described using a kernel function $K_n(x_0, t=0)$ associated with $\Delta\varphi$ [see Equation (26)]. The Rabi splitting thus depends not only on the position of the atom inside the cavity, but can also be imposed by the phase-difference of the paired laser-beams.

If the operative condition is close to that defined by Equation (36), such that $K_n(x_0, t=0) \approx 0$, the spectrum $W_n(x_0, \omega)$ as a function of the pure frequency ω is limited to two pulses that almost superimpose each other: 1) a Lorentzian function centred in the n^{th} QNM frequency $\operatorname{Re} \omega_n$, with bandwidth $2 | \operatorname{Im} \omega_n |$, superimposed on 2) a Dirac distribution of atomic resonance $\Omega \approx \operatorname{Re} \omega_n$, so that [see Equations (16)-(18)]

$$W_n(x_0, \omega) \approx \sigma_n^{(II)}(\omega) + \frac{\alpha_n''}{d} \delta(\omega - \Omega) \rightarrow \delta(\omega - \Omega), \quad (50)$$

when α_n'' is the normalization constant that satisfies condition (45). The two poles, ω_1 and ω_2 , can be simplified as [see Equations (14), (28) and (29)]:

$$\begin{aligned} \omega_1 &\approx \operatorname{Re} \omega_n + i \operatorname{Im} \omega_n \\ \omega_2 &\approx \Omega. \end{aligned} \quad (51)$$

7. Criteria for designing an active delay line

In references [23,24] and subsequent papers, the QNM theory was applied to a photonic crystal (PC) as a symmetric Quarter-Wave (QW) 1D-PBG cavity. The present study considers a symmetric QW 1D-PBG cavity with parameters $\lambda_{\text{ref}}=1\mu\text{m}$, $N=5$, $n_h=2$, $n_l=1.5$ (see Figure 1). The motivation for choosing this cavity is that it provides a relatively simple physical context for discussion of criteria in order to design an active delay line. An atom is located in the centre of the 1D-PBG, so that $x_0=d/2$ (see Figure 1). Reference [28] discusses how in a symmetric QW 1D-PBG cavity with reference wavelength ω_{ref} and N periods, the $[0, 2\omega_{\text{ref}}]$ range includes $2N + 1$ QNMs, which are identified as $|n\rangle$, $n \in [0, 2N]$ (with the exclusion of $\omega=2\omega_{\text{ref}}$). If the location of the atom is the centre x_0 of the 1D-PBG cavity, then it can only be coupled to one of the even QNMs n because the QNM intensity $|f_n|^2$ in this position has a maximum for even values of n and is almost null for odd values of n .

The active cavity consists of the 1D-PBG cavity containing one atom, and it is characterized by a $G(x_0, \omega)$ global transmission spectrum, this being the product of the 1D-PBG $|t(\omega)|^2$ transmission spectrum, and the $W(x_0, \omega)$ emission spectrum of the atom [in units of s], so

$$G(x_0, \omega) = W(x_0, \omega)|t(\omega)|^2 \text{ [in units of } s \text{]}. \tag{52}$$

It is possible to define the active cavity's "density of coupling" (DOC) $\sigma_c(x_0, \omega)$, as the probability density that an atom embedded at point x_0 is coupled to only a single QNM, with a oscillation close to the frequency ω . The DOC $\sigma_c(x_0, \omega)$ [in units of s^2/m] is the product of the atomic emission spectrum $W(x_0, \omega)$, and the DOS $\sigma(\omega)$ [in units of s/m]. It is possible to introduce an "acceleration of coupling" $a_c(x_0, \omega)$ inside the active cavity as:

$$a_c(x_0, \omega) = \frac{1}{\sigma_c(x_0, \omega)} = \frac{1}{W(x_0, \omega)\sigma(\omega)} = \frac{v(\omega)}{W(x_0, \omega)} \text{ [in units of } m / s^2 \text{]}. \tag{53}$$

when $v(\omega)=1/\sigma(\omega)$. If the active cavity is to be designed as an ideal delay line, then the pulsed input needs to be retarded and highly amplified, but free of any distortion. For a narrow pass band the global transmission (52) needs to be very high, with a quasi-constant acceleration of coupling (53).

As described above, an atom embedded in the centre of a symmetric QW 1D-PBG cavity with $N=5$ periods (Figure 1) can only be coupled to a single QNM, oscillating close to an even transmission peak $n=0,2,\dots,2N$. If it is assumed that the atom is coupled to the $(N+1)^{\text{th}}$ QNM, close to the edge of the high frequency band, then the 1D-PBG cavity quality factor will be

$$Q_{N+1} = \frac{\Omega}{|\text{Im}\omega_{N+1}|}, \tag{54}$$

when Ω is the atom's resonance frequency. If it is also assumed that a strong coupling regime is in force, then the active delay line directories can be satisfied by an appropriate coupling degree value,

$$R = \frac{\Gamma_0}{\Omega}, \quad (55)$$

when Γ_0 denotes the atomic decay rate in vacuum, and by a suitable atomic frequency detuning value - $(N+1)^{\text{th}}$ QNM coupling,

$$\Delta_{N+1} = \frac{\text{Re} \omega_{N+1} - \Omega}{R}. \quad (56)$$

If spontaneous emission occurs, assuming perfect tuning so that $\Delta_{N+1} = 0$, then the oscillation of the atom is at the frequency of the $(N+1)^{\text{th}}$ QNM, which is $\Omega = \text{Re} \omega_{N+1}$. A suitable value of coupling degree R thus exists (see Figures 2.a and 2.b) as $R^* = 0.002506$, making the two poles [Equations (29) and (22)] of the atomic emission spectrum distinct for $R > R^*$ or coincident for $0 < R < R^*$. Alternatively stated, when $R > R^*$, there is a Rabi splitting (see Figure 3.a) in the atomic emission spectrum [Equations (47), (48) and (22)], generating an oscillation (see Figure 4.a) in the atomic emission probability [Equations (34) and (22)]. Conversely, when $0 < R < R^*$, the emission spectrum comprises two superimposed peaks, indicating over-damping of the emission probability. In an attempt to identify Rabi splitting under strong coupling and consistent with experimentation ($\Gamma_0 \sim |\text{Im} \omega_{N+1}|$) [38], the following degree of coupling is postulated:

$$R = R_{N+1} = \frac{1}{Q_{N+1}}. \quad (57)$$

The two spontaneous emission spectrum poles, shifted by the atomic resonance Ω , are $\xi_1 = 0.06383 + i0.01770$ and $\xi_2 = -0.06383 + i0.01995$ in units of ω_{ref} (see Figures 2.a and 2.b). They describe the two emission spectrum peaks in resonance and bandwidth, with maxima of $W_1 = 21.87$ and $W_2 = 15.66$ in units of ω_{ref} (see Figure 3.a). Assuming the disappearance of emission probability after the second oscillation, then the decay time value is $\tau = 94.3$ in units of $1/\omega_{\text{ref}}$ (see Figure 4.a). The active cavity designed in this way is a less than ideal optical amplifier, in the sense that the amplification of an input pulse is accompanied by distortion. In the case of spontaneous emission plotted in Figures 5.a and 5.b the pass band is narrow, with $\xi = \omega - \Omega \approx (-0.06, 0.06)$ (in units of ω_{ref}), where the global transmission spectrum exhibits relatively high values, $G_{C,N+1} \in (G_{\text{min}}, G_{\text{max}}) = (2.881, 14.43)$ in units of $1/\omega_{\text{ref}}$. While the coupling acceleration is modulated close to the value $v_{C,N+1} = 0.03445$ in units of $\omega_{\text{ref}}/v_{\text{ref}}$.

An example of stimulated emission is now considered, with the atom inside the symmetric QW 1D-PBG cavity being excited by a pair of counter-propagating laser beams. The phase

difference $\Delta\varphi$ of the two laser beams can thus be added as a new degree of freedom for the realization of an active delay line. If perfect tuning is assumed during stimulated emission, when $\Delta_{\text{st}}=0$, the atom again oscillates at the frequency of the $(N+1)^{\text{th}}$ QNM, which is $\Omega=\text{Re}\omega_{N+1}$. The phase difference range $\Delta\varphi$, this being $(\Delta\varphi_1, \Delta\varphi_2)=(2.747, 3.524)$ in *rad* units, is adequate (see Figures 2.c and 2.d) to make the two poles [Equations (29) and (26)] of the atomic emission spectrum distinct for $\Delta\varphi<\Delta\varphi_1$ and $\Delta\varphi>\Delta\varphi_2$, but coincident for $\Delta\varphi_1<\Delta\varphi<\Delta\varphi_2$. In other terms, when $\Delta\varphi<\Delta\varphi_1$ and $\Delta\varphi>\Delta\varphi_2$ Rabi splitting (see Figure 3.a) occurs in the atomic emission spectrum [Equations (47), (48) and (26)], with an oscillation (see Figure 4.a) in the probability of atomic emission [Equations (35) and (26)]. When $\Delta\varphi_1<\Delta\varphi<\Delta\varphi_2$, the emission spectrum comprises two superimposed peaks with over-damping of emission probability. The Rabi splitting and decay time oscillations can therefore be controlled using the phase difference of the paired laser beams.

Using stimulated emission to obtain an ideal delay line, requires that the paired laser beams have higher quadrature, so $\Delta\varphi>\pi/2$. Compared to spontaneous emission, the emission spectrum must show narrower Rabi splitting and the emission probability must have a longer decay time. The active cavity comprising the 1D-PBG together with the atom can thus act as a delay line, because the active cavity delay time is linked to the atomic decay time (for examples, see references [39-41]). As noted above, then it is necessary that the phase difference remains within a maximum of $\Delta\varphi_1=2.747$ (in *rad* units), beyond which the Rabi splitting tends towards zero. In the same time domain, increasing the phase difference relative to $\Delta\varphi \approx \pi/2$, causes the decay time to become even longer, while in the frequency domain the global transmission (52) exhibits high gain but instead the acceleration of coupling (53) exhibits a narrow pass band. The active cavity thus acts as an active but not ideal delay line when $\Delta\varphi \rightarrow \Delta\varphi_1$. This leads to the conclusion that the 1D-PBG cavity should be pumped by paired laser beams exceeding a tilt angle quadrature of:

$$\Delta\varphi = \frac{\pi}{2} + \frac{\pi}{10}. \tag{58}$$

The two stimulated emission spectrum poles are shifted by the resonance Ω , and are respectively $\xi_1=0.05205+i0.01787$ and $\xi_2=-0.05205+i0.01978$ (in units of ω_{ref}) (see Figures 2.c and 2.d). The two poles are closer by $\Delta\xi=0.02356$ compared to spontaneous emission. They describe the resonance and band width of the two stimulated emission spectrum peaks, with maxima of $W_1=14.36$ and $W_2=10.93$ (in units of ω_{ref}) (see Figure 3.a). Compared to spontaneous emission, the two maxima are reduced by $\Delta W_1=7.51$ and $\Delta W_2=4.73$. If an emission probability of almost zero is assumed after the second oscillation, then the stimulated emission decay time is $\tau=113.5$ (in units of $1/\omega_{\text{ref}}$) (see Figure 4.a). Compared to spontaneous emission, this time is increased by $\Delta\tau=19.2$. The phase difference of the two laser beams thus enables control of atomic decay time and of active cavity delay time [39-41]. At this point a less than ideal delay line has been designed, in which an input pulse is retarded and amplified but somewhat distorted. The plots of Figures 5.a and 5.b show that, compared to spontaneous emission, there is a narrower pass band, with $\xi = \omega-\Omega \approx (-0.04, 0.04)$, with the global transmission spectrum exhibiting similar

values, so $G_{C,N+1} \in (G_{\min}, G_{\max}) = (3.270, 9.24)$ (in units of ω_{ref}), and most significantly the acceleration of coupling is now slightly modulated around the value $v_{C,N+1} = 0.05310$ (in units of $\omega_{\text{ref}}/v_{\text{ref}}$).

Finally, stimulated emission is considered in the presence of a degree of detuning, when the atom inside the symmetric QW 1D-PBG cavity remains coupled to the $(N+1)^{\text{th}}$ QNM, but no longer oscillates at the $(N+1)^{\text{th}}$ QNM frequency. The active delay line design can be improved with a final degree of freedom by varying the frequency detuning of the atom - $(N+1)^{\text{th}}$ QNM coupling (56). The application of maximum detuning is proposed to improve the active delay line. The atomic resonance Ω is lowered to within the photonic band gap, close to the $(N+1)^{\text{th}}$ QNM frequency $\text{Re}\omega_{N+1}$, and the atom only remains coupled to the $(N+1)^{\text{th}}$ QNM if the atomic resonance is within the limit

$$\Omega = \text{Re}\omega_{N+1} - |\text{Im}\omega_{N+1}|, \quad (59)$$

when detuning is maximum:

$$\Delta_{N+1} = \frac{\text{Re}\omega_{N+1} - \Omega}{R_{N+1}} = \frac{|\text{Im}\omega_{N+1}|}{R_{N+1}}. \quad (60)$$

Detuned in this way, the two stimulated emission spectrum poles are shifted by the resonance Ω and exhibit real parts $\text{Re}\xi_1 = 0.03738$ and $\text{Re}\xi_2 = -0.07380$, and imaginary parts $\text{Im}\xi_1 = 0.01176$ and $\text{Im}\xi_2 = 0.02588$ (both in units of ω_{ref}) (see Figures 2.c and 2.d). Compared to perfect tuning, the real parts are reduced by $\Delta\text{Re}\xi_1 = 0.01467$ and $\Delta\text{Re}\xi_2 = 0.02175$, while one imaginary part is reduced by $\Delta\text{Im}\xi_1 = 0.00611$ and the other is raised by $\Delta\text{Im}\xi_2 = 0.0061$. They describe the resonance and bandwidth of the two peaks of the stimulated emission spectrum when detuned, with maxima of $W_1 = 38.83$ and $W_2 = 0.2974$ (in units of ω_{ref}) (see Figure 3.b). Compared to perfect tuning, the first peak is raised by $\Delta W_1 = 24.47$ and the second peak is lowered by $\Delta W_2 = 10.63$. If the atomic emission probability is assumed to be almost zero after the second oscillation, then the stimulated emission decay time (linked to the active cavity delay time) in the detuned example is $\tau = 111.2$ (in units of $1/\omega_{\text{ref}}$) (see Figure 4.b). Compared to perfect tuning, the emission probability (and thus the input pulse) is somewhat warped and retarded by $\Delta\tau = 2.3$.

The result is the design of a close to ideal delay line, with an input pulse being retarded, amplified and only slightly distorted. The plots of Figures 5.c and 5.d show that compared to stimulated emission, the detuned example has an even narrower pass band, at $\xi = \omega - \Omega \approx (0.02, 0.06)$, with the global transmission spectrum exhibiting higher values, with $G_{C,N+1} \in (G_{\min}, G_{\max}) = (6.005, 36.77)$ (in units of $1/\omega_{\text{ref}}$). Most significantly, the coupling acceleration is completely no modulated and almost constant at $v_{C,N+1} \cong 0.007182$ (in units of $\omega_{\text{ref}}/v_{\text{ref}}$). As seen in Figure 5.d, the coupling acceleration modulation is shifted into the unused frequency range $\xi \approx (-0.07, -0.04)$.

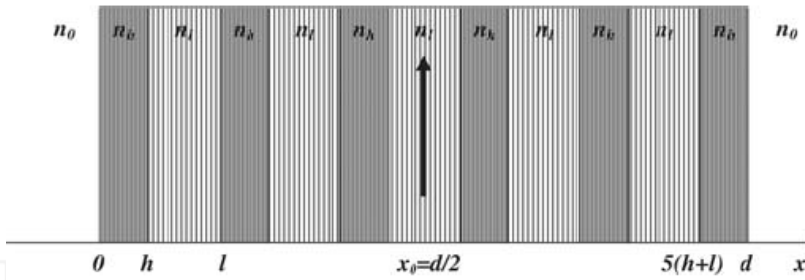


Figure 1. Symmetric Quarter-Wave (QW) one dimensional (1D) Photonic Band Gap (PBG) cavity with $\lambda_{\text{ref}}=1\mu\text{m}$ as reference wavelength, $N=5$ periods, consisting of two layers with refractive indices $n_h=2$ and $n_l=1.5$ and lengths $h=\lambda_{\text{ref}}/4n_h$ and $l=\lambda_{\text{ref}}/4n_l$. Terminal layers of the symmetric QW 1D-PBG cavity with parameters: n_h and $h=\lambda_{\text{ref}}/4n_h$. Length of the 1D-PBG cavity: $d=N(h+l)+h$. One atom is present, embedded in the centre of the 1D-PBG, so that $x_0=d/2$ (Figure reproduced from references [32,33]).

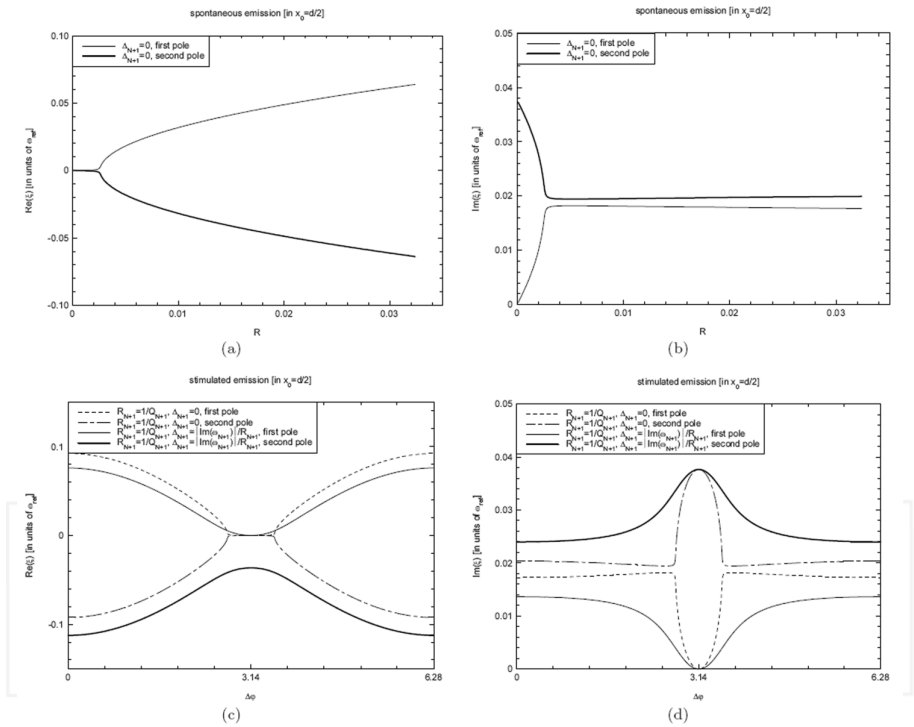


Figure 2. If the atom embedded inside the 1D-PBG cavity of Figure 1 oscillates at the $(N+1)^{\text{th}}$ Quasi-Normal Mode (QNM), close to the high-frequency band limit [i.e. perfectly tuned $\Delta_{\text{N},1}=0$, see Equation (56)], spontaneous emission under strong coupling regime exhibit two characteristic atomic emission spectrum poles, each pole being shifted by the atomic resonance Ω [see Equations (29) and (22)]; the real (Figure 2.a) and imaginary (Figure 2.b) parts, in units of the 1D-PBG reference frequency ω_{ref} are plotted as functions of the degree of coupling $R=\gamma/\Omega$, this being the ratio between the atomic decay-rate in vacuum γ and resonance Ω [see Equation (55)].

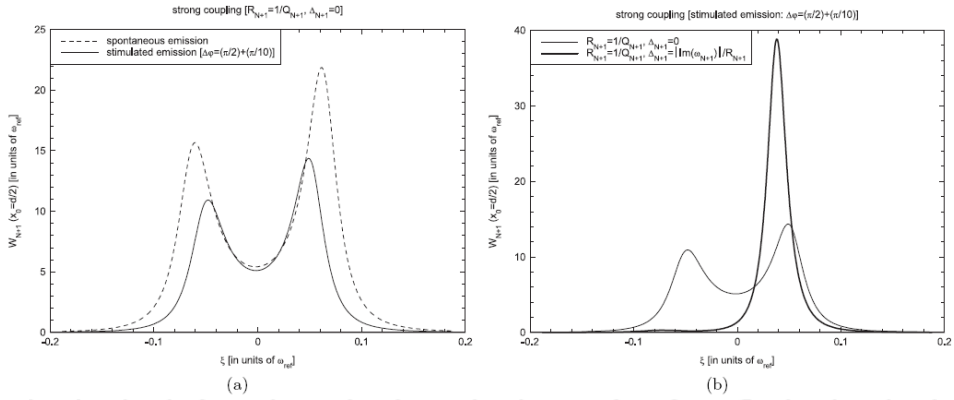


Figure 3. The emission spectrum of the atom embedded inside the 1D-PBG cavity of Figure 1 is plotted in units of the 1D-PBG reference frequency ω_{ref} and as a function of the dimensionless shifted frequency $\xi = (\omega - \Omega) / \omega_{ref}$ with Ω denoting atomic resonance. The atom is coupled to the $(N+1)^{th}$ QNM frequency and emission occurs under strong coupling regime [for $R_{N+1} = 1/Q_{N+1}$]. Figure 3.a illustrates hypothetical tuning, with the spontaneous atomic emission spectrum [see Equations (47) and (48)] compared to the stimulated emission spectrum [see Equations (47) and (48)], when the 1D-PBG is pumped by paired laser beams with an appropriate phase difference: $\Delta\varphi = (\pi/2) + (\pi/10)$ [see Equation (58)]. Figure 3.b instead illustrates a case of stimulated emission, comparing the perfectly tuned atomic emission spectrum with the detuned emission spectrum (Figure reproduced from references [32,33]).

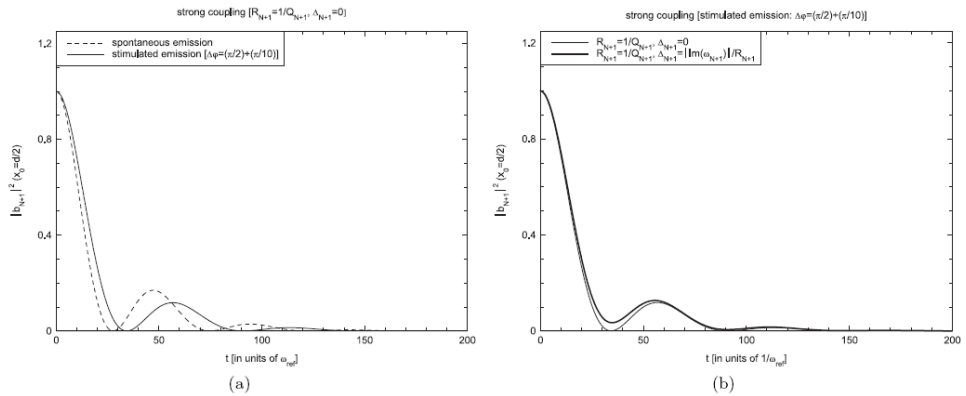


Figure 4. The emission probability of the atom embedded inside the 1D-PBG cavity of Figure 1 is plotted as a function of the normalized time $\omega_{ref} t$, with ω_{ref} being the 1D-PBG reference frequency. With reference to the operative conditions of Figure 3: hypothetical tuning is shown in Figure 4.a, comparing the spontaneous atomic emission probability [see Equation (34)], with stimulated emission probability [see Equation (35)] when the 1D-PBG is pumped by paired laser beams with an appropriate phase difference: $\Delta\varphi = (\pi/2) + (\pi/10)$. Figure 4.b illustrates stimulated emission, comparing atomic emission probability under perfect tuning with emission probability when detuned (Figure reproduced from references [32,33]).

If a pair of counter-propagating laser beams are tuned to the resonance Ω and the atom is coupled to the $(N+1)^{th}$ QNM, [i.e. $Q_{N+1} = \Omega / \text{Im}\omega_{N+1}$, see Equation (54)], the stimulated emission

under strong coupling [for $R_{N+1} = 1/Q_{N+1}$, see Equation (57)] exhibits two characteristic atomic emission spectrum poles, each pole being shifted by the resonance Ω [see Equations (29) and (26)]. The real (Figure 2.c) and imaginary (Figure 2.d) parts, in units of the 1D-PBG reference frequency ω_{ref} are plotted as functions of the phase difference $\Delta\varphi$ between the paired laser beams regardless of whether the atom oscillates at the $(N+1)^{th}$ QNM frequency [i.e. perfectly tuned $\Delta_{N+1} = 0$] or at a frequency in the band gap close to the high frequency band limit [i.e. detuned $\Delta_{N+1} = \text{Im}\omega_{N+1} / R_{N+1}$, see Equation (60)] (Figure reproduced from references [32,33]).

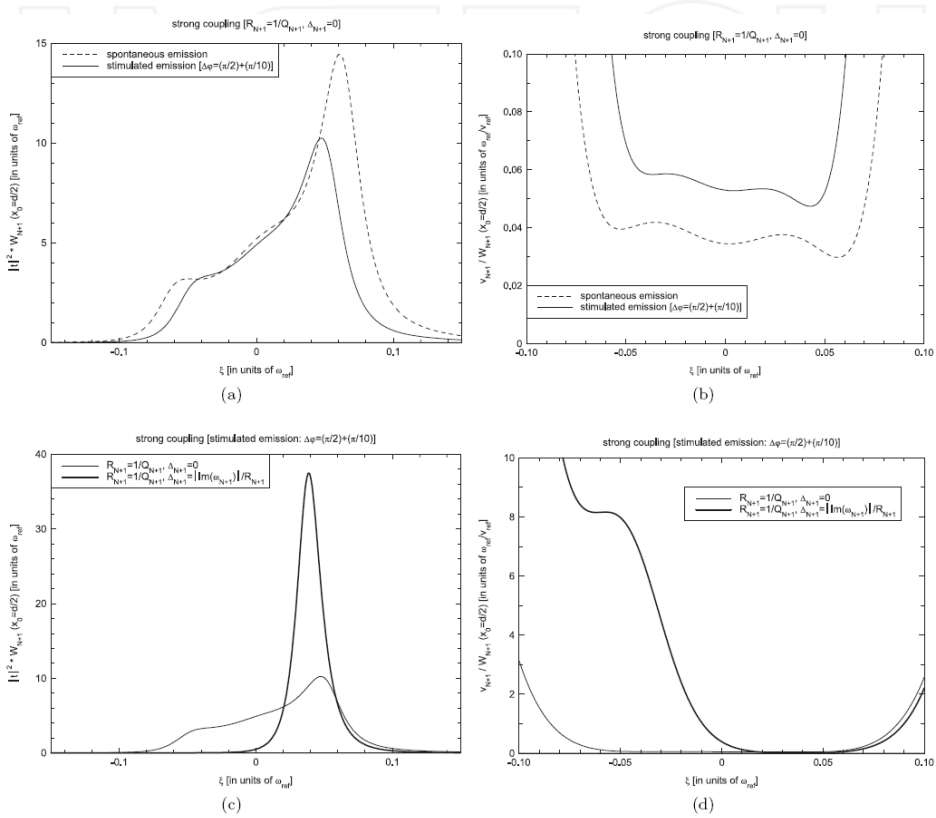


Figure 5. A delay line using an active cavity comprising the 1D-PBG cavity plus atom (Figure 1) can be designed by characterizing the line according to global transmission [see Equation (52)], and “coupling acceleration” [see Equation (53)] of the electromagnetic (e.m.) field. Global transmission, in units of the 1D-PBG reference frequency ω_{ref} and coupling acceleration, in units of ω_{ref}/v_{ref} being v_{ref} the group velocity of the e.m. field in vacuum, are plotted as functions of the dimensionless shifted frequency $\xi = (\omega - \Omega) / \omega_{ref}$ with Ω denoting atomic resonance. With reference to the operative conditions of Figure 3: perfect tuning is shown in Figure 5.a (Figure 5.b), comparing the global transmission (coupling acceleration) of the active delay line for spontaneous emission, with the global transmission (coupling acceleration) for stimulated emission when the 1D-PBG is pumped by paired laser beams with an appropriate phase difference: $\Delta\varphi = (\pi/2) + (\pi/10)$. Figure 5.c (Figure 5.d) compares the global transmission (coupling acceleration) of the active delay line when perfectly tuned, with the global transmission (coupling acceleration) when detuned under stimulated emission (Figure reproduced from references [32,33]).

8. Final discussion and concluding remarks

This chapter discussed atomic stimulated emission processes, under strong coupling, inside a one dimensional (1D) Photonic Band Gap (PBG) cavity, which is pumped by a pair of counter-propagating laser beams [32,33]. The atom-field interaction was modelled by quantum electrodynamics, with the atom considered as a two level system, the electromagnetic (e.m.) field as superposition of its normal modes, and applying the dipole approximation, the Wigner-Weisskopf equations of motion, and the rotating wave approximations. The unenclosed cavity example under investigation was approached applying the Quasi-Normal Mode (QNM), while the local density of states (LDOS) was interpreted as the local probability density of exciting a single QNM within the cavity. In this approach, the LDOS depends on the phase difference of the paired laser beams, and the most significant result is that the strong coupling regime can occur with high LDOS values. The investigation also confirms the well known phenomenon [39-41] that atomic emission probability decays with oscillation, causing the atomic emission spectrum to split into two peaks (Rabi splitting). The novelty that emerged in this chapter is that it appears to be possible to coherently control both the atomic emission probability oscillations and the Rabi splitting of the emission spectrum using the phase difference of the paired laser beams. Finally, some criteria were proposed for the design of an active cavity comprising a 1D-PBG cavity plus atom, to serve as an active delay line. It is seen that suitable phase differences between the paired laser beams make it possible to achieve high delayed pulse transmission in a narrow pass band.

The issue of e.m. field interaction with atoms when the e.m. modes are conditioned by the environment (inside a cavity, or proximal to walls) can be approached in several ways. For example, the dynamics of the e.m. field can first be established inside and outside the cavity (or proximal/distant from walls), and then atomic coupling with the normal modes (NMs) of the combined system [42-46] can be considered. An alternative approach applies the discrete (dissipative) QNMs of the unenclosed cavity in place of the continuous (Hermitian) NMs. When applying the QNMs, the internal field cavity is coupled to the external e.m. fields (beyond the two cavity limits) by boundary conditions [47-50].

A third approach is proposed in the present chapter, combining both those described above with the aim of merging their analytic potentials. Canonical quantum electro-dynamics is applied for the definition of an e.m field as a superposition of NMs, while an unenclosed cavity is defined adopting a QNM approach, when LDOS is interpreted as the local probability density of exciting a single QNM of the cavity. The DOS is linked to the cavity boundary conditions. The e.m. field satisfies incoming and outgoing wave conditions on the cavity surfaces, and so the DOS depends on the externally pumped photon reservoir. When the cavity is excited by paired counter-propagating pumps, the DOS expresses the probability distribution of exciting a single QNM of the cavity.

In the case of spontaneous emission, the paired pumps are modelled as vacuum fluctuations from the ground state of the e.m. field, while the DOS is construed simply as a feature of cavity geometry. Instead, in the case of stimulated emission, the paired pumps are modelled as two laser beams in a coherent state, so that the DOS depends on the cavity geometry and can be

controlled by the phase difference of the paired laser beams. These results clearly highlight how the DOS of an unenclosed cavity is determined by the cavity excitation state.

Acknowledgements

The author, Dr. Alessandro Settimi, is extremely grateful to Dr. Sergio Severini for his outstanding support and friendship, to Prof. Concita Sibilgia and Prof. Mario Bertolotti for their interesting pointers to literature regarding photonic crystals, and to Prof. Anna Napoli and Prof. Antonino Messina for their valuable discussions regarding stimulated emission.

Author details

Alessandro Settimi*

Address all correspondence to: alessandro.settimi@ingv.it

Istituto Nazionale di Geofisica e Vulcanologia (INGV), Sezione di Geomagnetismo, Aeronomia e Geofisica Ambientale (ROMA 2), Rome, Italy

References

- [1] Purcell E. M. Spontaneous emission probabilities at radio frequencies. *Physical Review* 1946; 69, 681.
- [2] Kleppner D. Inhibited Spontaneous Emission. *Physical Review Letters* 1981; 47 (4) 233-236, DOI: /10.1103/PhysRevLett.47.233.
- [3] Drexhage K. H. Interaction of light with monomolecular dye layers. In: Wolf E. (ed.) *Progress in Optics*. New York: North-Holland; 1974. vol. 12, p. 165.
- [4] Goy P., Raimond J. M., Gross M., Haroche S. Observation of Cavity-Enhanced Single-Atom Spontaneous Emission. *Physical Review Letters* 1983; 50 (24) 1903-1906, DOI: 10.1103/PhysRevLett.50.1903.
- [5] Hulet R. G., Hilfer E. S., Kleppner D. Inhibited Spontaneous Emission by a Rydberg Atom. *Physical Review Letters* 1985; 55 (20) 2137-2140, DOI: 10.1103/PhysRevLett.55.2137.
- [6] Jhe W., Anderson A., Hinds E. A., Meschede D., Moi L., Haroche S. Suppression of spontaneous decay at optical frequencies: Test of vacuum-field anisotropy in confined space. *Physical Review Letters* 1987; 58 (7) 666-669, DOI: 10.1103/PhysRevLett.58.666.

- [7] Heinzen D. J., Childs J. J., Thomas J. E., Feld M. S. Enhanced and inhibited visible spontaneous emission by atoms in a confocal resonator. *Physical Review Letters* 1987; 58 (13) 1320-1323, DOI: 10.1103/PhysRevLett.58.1320.
- [8] De Martini F., Innocenti G., Jacobovitz G. R., Mataloni P. Anomalous Spontaneous Emission Time in a Microscopic Optical Cavity. *Physical Review Letters* 1987; 59 (26) 2955-2928, DOI: 10.1103/PhysRevLett.59.2955.
- [9] Jaynes E. T., Cummings F. W. Comparison of quantum and semiclassical radiation theories with application to the beam maser. *Proceedings of the IEEE* 1963; 51 (1) 89-109, DOI: 10.1109/PROC.1963.1664.
- [10] Rempe G., Walther H., Klein N. Observation of quantum collapse and revival in a one-atom maser. *Physical Review Letters* 1987; 58 (4) 353-356, DOI: 10.1103/PhysRevLett.58.353.
- [11] John S. Electromagnetic Absorption in a Disordered Medium near a Photon Mobility Edge. *Physical Review Letters* 1984; 53 (22) 2169-2172, DOI: 10.1103/PhysRevLett.53.2169.
- [12] Yablonovitch E. Inhibited Spontaneous Emission in Solid-State Physics and Electronics. *Physical Review Letters* 1987; 58 (20) 2059-2062, DOI: 10.1103/PhysRevLett.58.2059.
- [13] John S. Strong localization of photons in certain disordered dielectric superlattices. *Physical Review Letters* 1987; 58 (23) 2486-2489, DOI: 10.1103/PhysRevLett.58.2486.
- [14] John S., Wang J. Quantum electrodynamics near a photonic band gap: Photon bound states and dressed atoms. *Physical Review Letters* 1990; 64 (20) 2418-2421, DOI: 10.1103/PhysRevLett.64.2418.
- [15] John S., Wang J. Quantum optics of localized light in a photonic band gap. *Physical Review B* 1991; 43 (16) 12772-12789, DOI: 10.1103/PhysRevB.43.12772.
- [16] Burstein E., Weisbuch C., editors. *Confined Electrons and Photons: New Physics and Applications*. New York: Plenum Press; 1995. p. 907.
- [17] Nabiev R. F., Yeh P., Sanchez-Mondragon J. J. Dynamics of the spontaneous emission of an atom into the photon-density-of-states gap: Solvable quantum-electrodynamical model. *Physical Review A* 1993; 47 (4) 3380-3384, DOI: 10.1103/PhysRevA.47.3380.
- [18] Lai H. M., Leung P. T., Young K. Electromagnetic decay into a narrow resonance in an optical cavity. *Physical Review A* 1988; 37 (5) 1597-1606, DOI: 10.1103/PhysRevA.37.1597.
- [19] Leung P. T., Liu S. Y., Young K. Completeness and orthogonality of quasinormal modes in leaky optical cavities. *Physical Review A* 1994; 49 (4) 3057-3067, DOI: 10.1103/PhysRevA.49.3057.
- [20] Leung P. T., Tong S. S., Young K. Two-component eigenfunction expansion for open systems described by the wave equation I: completeness of expansion. *Journal of*

- Physics A: Mathematical and General 1997; 30 (6) 2139-2151, DOI: 10.1088/0305-4470/30/6/034.
- [21] Leung P. T., Tong S. S., Young K. Two-component eigenfunction expansion for open systems described by the wave equation II: linear space structure. *Journal of Physics A: Mathematical and General* 1997; 30 (6) 2153-2162, DOI: 10.1088/0305-4470/30/6/035.
- [22] Ching E. S. C., Leung P. T., Maassen van der Brink A., Suen W. M., Tong S. S., Young K. Quasinormal-mode expansion for waves in open systems. *Reviews of Modern Physics* 1998; 70 (4) 1545-1554, DOI: 10.1103/RevModPhys.70.1545.
- [23] Settimi A., Severini S., Mattiucci N., Sibilia C., Centini M., D'Aguanno G., Bertolotti M., Scalora M., Bloemer M., Bowden C. M. Quasinormal-mode description of waves in one-dimensional photonic crystals. *Physical Review E* 2003; 68 (2) 026614 [1-11], DOI: 10.1103/PhysRevE.68.026614.
- [24] Severini S., Settimi A., Sibilia C., Bertolotti M., Napoli A., Messina A. Quasi-Normal Frequencies in Open Cavities: An Application to Photonic Crystals. *Acta Physica Hungarica B* 2005; 23 (3-4) 135-142, DOI: 10.1556/APH.23.2005.3-4.3.
- [25] Cohen-Tannoudji C., Diu B., Laloe F. *Quantum Mechanics*. New York: John Wiley & Sons Inc., Second Volume Set Edition; 1977. p. 1524.
- [26] Louisell W. H. *Quantum Statistical Properties of Radiation (Pure & Applied Optics)*. New York: John Wiley & Sons Inc., First Edition; 1973. p. 544.
- [27] Ho K. C., Leung P. T., Maassen van den Brink A., Young K. Second quantization of open systems using quasinormal modes. *Physical Review E* 1998; 58 (3) 2965-2978, DOI: 10.1103/PhysRevE.58.2965.
- [28] Severini S., Settimi A., Sibilia C., Bertolotti M., Napoli A., Messina A. Second quantization and atomic spontaneous emission inside one-dimensional photonic crystals via a quasinormal-modes approach. *Physical Review E* 2004; 70 (5) 056614, [1-12], DOI: 10.1103/PhysRevE.70.056614.
- [29] Severini S., Settimi A., Sibilia C., Bertolotti M., Napoli A., Messina A. Coherent control of stimulated emission inside one dimensional photonic crystals: strong coupling regime. *European Physical Journal B* 2006; 50 (3) 379-391, DOI: 10.1140/epjb/e2006-00165-2.
- [30] Severini S., Settimi A., Sibilia C., Bertolotti M., Napoli A., Messina A. Erratum - Coherent control of stimulated emission inside one dimensional photonic crystals: strong coupling regime. *European Physical Journal B* 2009; 69 (4) 613-614, DOI: 10.1140/epjb/e2009-00201-9.
- [31] Settimi A., Severini S., Sibilia C., Bertolotti M., Centini M., Napoli A., Messina A. Coherent control of stimulated emission inside one-dimensional photonic crystals. *Physical Review E* 2005; 71 (6) 066606 [1-10], DOI: 10.1103/PhysRevE.71.066606.

- [32] Settimi A., Severini S., Sibilia C., Bertolotti M., Napoli A., Messina A.. Coherent control of stimulated emission inside one dimensional photonic crystals: strong coupling regime. *European Physical Journal B* 2006; 50 (3) 379-391, DOI: 10.1140/epjb/e2006-00165-2.
- [33] Settimi A., Severini S., Sibilia C., Bertolotti M., Napoli A., Messina A.. ERRATUM Coherent control of stimulated emission inside one dimensional photonic crystals: strong coupling regime. *European Physical Journal B* 2009; 69 (4) 613-614, DOI: 10.1140/epjb/e2009-00201-9.
- [34] Abrikosov A. A., Gor'kov L. P. Dzyaloshinski I. E. *Methods of Quantum Field Theory in Statistical Physics (Dover Books on Physics)*. New York: Dover Publications, Revised Edition; 1975. p. 384.
- [35] Leung P. T., Maassen van den Brink A., Young K. Quasinormal-mode Quantization of Open Systems. In: Lim S. C., Abd-Shukor R., Kwek K. H. (eds) *Frontiers in Quantum Physics: proceedings of the International Conference, July 1998, University Kelangsoo, Singapore, Malaysia*. Singapore: Springer-Verlag; 1998. p. 214-218.
- [36] Blow K. J., Loudon R., Phoenix S. J. D., Shepherd T. J. Continuum fields in quantum optics. *Physical Review A* 1990; 42 (7) 4102-4114, DOI: 10.1103/PhysRevA.42.4102.
- [37] Carrier G. F., Krook M., Pearson C. E. *Functions of a complex variable – theory and technique*. New York: McGraw-Hill Book Company, First Edition; 1966. p. 438.
- [38] Hughes S., Kamada H. Single-quantum-dot strong coupling in a semiconductor photonic crystal nanocavity side coupled to a waveguide. *Physical Review B* 2004; 70 (19) 195313 [1-5], DOI: 10.1103/PhysRevB.70.195313.
- [39] Allen L., Eberly, J. H. *Optical Resonance and Two-Level Atoms (Dover Books on Physics)*. New York: Dover Publication; 1987. p. 256.
- [40] Bonifacio R., Lugiato L. A. Cooperative radiation processes in two-level systems: Superfluorescence. *Physical Review A* 1975; 11 (5) 1507-1521, DOI: 10.1103/PhysRevA.11.1507.
- [41] Sakoda K., Haus J. W. Superfluorescence in photonic crystals with pencil-like excitation. *Physical Review A* 2003; 68 (5) 053809 [1-5], DOI: 10.1103/PhysRevA.68.053809.
- [42] Louisell W. H., Walker L. R. Density-Operator Theory of Harmonic Oscillator Relaxation. *Physical Review* 1965; 137 (1B) B204-B211, DOI: 10.1103/PhysRev.137.B204.
- [43] Senitzky I. R. Dissipation in Quantum Mechanics. *The Harmonic Oscillator*. *Physical Review* 1960; 119 (2) 670-679, DOI: 10.1103/PhysRev.119.670.
- [44] Senitzky I. R. Dissipation in Quantum Mechanics. *The Harmonic Oscillator*. II. *Physical Review* 1961; 124 (3) 642-648, DOI: 10.1103/PhysRev.124.642.
- [45] Senitzky I. R. Dissipation in Quantum Mechanics. *The Two-Level System*. *Physical Review* 1963; 131 (6) 2827-2838, DOI: 10.1103/PhysRev.131.2827.

- [46] Lax M. Quantum Noise. IV. Quantum Theory of Noise Sources. *Physical Review* 1966; 145 (1) 110-129, DOI: 10.1103/PhysRev.145.110.
- [47] Dekker H. A note on the exact solution of the dynamics of an oscillator coupled to a finitely extended one-dimensional mechanical field and the ensuing quantum mechanical ultraviolet divergence. *Physics Letters A* 1984; 104 (2) 72-76, DOI: 10.1016/0375-9601(84)90965-4.
- [48] Dekker H. Particles on a string: Towards understanding a quantum mechanical divergence. *Physics Letters A* 1984; 105 (8) 395-400, DOI: 10.1016/0375-9601(84)90715-1.
- [49] Dekker H. Bound electron dynamics: Exact solution for a one-dimensional oscillator-string model. *Physics Letters A* 1984; 105 (8) 401-406, DOI: 10.1016/0375-9601(84)90716-3.
- [50] Dekker H. Exactly solvable model of a particle interacting with a field: The origin of a quantum-mechanical divergence. *Physical Review A* 1985; 31 (2) 1067-1076, DOI: 10.1103/PhysRevA.31.1067.

INTECH

